

Theoretical study of structural, electronic, and thermal properties of $\text{Cr}_2(\text{Zr}, \text{Nb})$ Laves alloys

A. Kellou¹, T. Grosdidier², C. Coddet¹, and H. Aourag¹

¹ LERMPS, Université de Belfort-Monbéliard,
90010 Belfort, France

² Laboratoire d'Etude des Textures et Application aux Matériaux, UMR CNRS 7078,
Université de Metz, Ile du Saulcy, 57045 Metz Cedex 01, France

Abstract

The Full-Potential Linearized Augmented Plane Waves (FP-LAPW) method using the Generalized Gradient Approximation (GGA) within the framework of Density functional Theory (DFT) is applied to study the lattice parameters, bulk moduli, and densities of states (DOS) of Cr_2Zr , Cr_2Nb , and their $\text{Cr}_2\text{Zr}_{1-x}\text{Nb}_x$ ternary alloys in the C15-Laves structure. The quasi-harmonic Debye model, using a set of total energy versus molar volume obtained with the FP-LAPW method, is applied to study the thermal and vibrational effects. Temperature effect on the structural parameters, thermal expansions, heat capacities, Grüneisen parameters, and Debye temperatures are determined from the non-equilibrium Gibbs functions and compared to available data.

Keywords: Ternary alloy systems, Laves phases, Thermal properties, Ab-initio calculations.

1. Introduction

Various intermetallic phases are being developed as new structural materials for high temperature applications. The familiar aluminides (Ti, Al or Fe based) are promising candidates for applications up to about 1000°C. Other less common intermetallic phases, such as the Laves phases, are looked upon for much higher temperatures. Laves structures are indeed characterized by high melting points that could bring a promising potential field for applications in aerospace and technological sectors^{1,2}. Of particular interest are the Cr_2X (X=Zr, Nb) compounds which have high creep and good oxidation resistances²⁻⁵. However, the cubic MgCu_2 -type structure (C15) of these compounds, which occurs at the stoichiometric composition, is very hard and extremely brittle at ambient temperatures⁴⁻⁶. One potential solution to this problem is the use an in-situ composite consisting of a ductile matrix phase, to provide toughness, reinforced by the Cr_2X Laves phase. For example, chromium-based alloys containing the Laves phase Cr_2X have recently been the subject of several investigations⁷⁻¹¹. Another potential interest of the Cr_2Nb phase is to be used as a stable precipitation for high temperature strength good conductivity Cu-based alloys¹².

Several theoretical and experimental studies have been devoted to these materials in order to understand the phase transformation, deformation, fracture, cracking behavior, oxidation resistance, phase stability, elastic properties, thermal stress, ...etc¹³⁻²¹. For example, the microstructure, cracking behaviour, thermal expansion, and mechanical properties of Laves phases in binary Cr–Nb, Cr–Zr and ternary Cr–(Nb, Zr) alloys were the subject of several investigations²²⁻²⁵. Also, elastic constants, Young's moduli, Poisson's ratios, sound velocities, and thermal expansion coefficients of $M\text{Cr}_2$ ($M=\text{Ti, Zr, Ta, Nb, Sc, Y, La}$) were obtained via a theoretical approach based on the Linear Muffin-Tin Orbital (LMTO-NFP) method; showing that DFT calculations can give satisfactory values that would often be difficult to obtain directly from

experiments^{25, 26}. Although several calculation methods have been successively applied to predict the stable ground state structure of various Laves phases, these calculations are: (i) always limited to the binary stoichiometric compounds and (ii) very often restricted to 0 K²⁷.

In order to avoid these limitations, the Full Potential Linearized Augmented Plane Waves (FP-LAPW) method is applied in the present work to investigate the structural and electronic properties of ternary alloys in the C15-Laves phase. In addition, the quasi-harmonic Debye model, which is added within the framework of the FP-LAPW, is used to reproduce the temperature effects. Thus, the aim of this work is threefold: (i) testing the validity of the quasi-harmonic Debye model using the total energy and molar volume set obtained with the FP-LAPW method and making it suitable for a large number of solids, (ii) highlighting the stability of ternary C15-Laves alloys for the Cr-Zr-Nb system, and (iii) giving electronic and vibrational properties of this phase since there is a lack in experimental data.

The parameters and technical details of the calculations related to the FP-LAPW method and the quasi-harmonic Debye model are presented in the second section of this paper. The results are given and discussed in the third section within two subsections dealing successively with: (i) the structural and electronic properties and (ii) the thermal effects. Finally, the fourth section gives some concluding remarks.

2. Computational methods

All calculations in this study are done within the framework of the density functional theory (DFT), according to which the many-body problem of interacting electrons and nuclei is mapped to a series of one-electron equations, the so-called Kohn–Sham (KS) equations. The self-consistent calculations were carried out for all structures using a scalar-relativistic version of the Full-Potential Linearized Plane Waves (FP-LAPW) method²⁸. The GGA approximation of Perdew *et al*²⁹ (PBE) to the local density approximation was taken to include the exchange-correlation energy to the total energy. Inside the muffin-tin spheres, the wavefunctions, electron charge densities, and potentials are expanded in terms of the spherical harmonics, while for the interstitial region between the spheres plane-wave expansions are used. The spherical harmonics were expanded up to angular momenta $l_{max} = 8$ inside the muffin-tin and $l_{max} = 4$ for the interstitial region, to avoid any shape approximations. The core states were treated fully relativistically in the frozen core approximation and the muffin-tin radii were taken as 2.10, 2.20, and 2.25 *a. u.* for Cr, Zr, and Nb, respectively. The present calculations were done without spin-orbit coupling (SOC).

Laves phases generally crystallize into one of the three topologically close-packed structures: cubic C15 (CuMg₂), hexagonal C14 (MgZr₂), and C36 (MgNi₂). As the Laves phases are stabilized by size factor principles and electronic structure, the *e/a* ratio - defined, for transition elements, as the average number of (*p* + *d*) electrons per atom - was identified as a key parameter in controlling the C14/C15 phase stability in Cr₂Nb based transition-metal Laves alloys³⁰. The lattice structure used in the calculations for the Cr₂Zr and Cr₂Nb compounds is similar to the Cu₂Mg cubic Laves structure (C15) having a Space Group: *Fd3m* (# 227). The C15 Laves phases have composition AB₂, where the A atoms are ordered as in diamond, and the B atoms form tetrahedra around the A atoms. The Cr(Zr, Nb) structures used in the calculation are like Cu₄MgSn (F-

43m, #216), which is an ordered variant of the Cu₂Mg structure. The 8-atom equipoint of the Cr₂Mg type structure is subdivided into two different, ordered, 4-point subsets in the Cu₄MgSn structure. This structure is one of the most commonly observed Laves phases among the known ternary systems.

The correct temperature variation of the thermal properties can only be obtained by treating the lattice vibrations as quantized (phonons). The investigations of thermal effects in this study are done within the quasi-harmonic Debye theory of crystals, without having to make extensive and complicated lattice dynamics calculations.

The isotropic approximation is used to determine the Debye temperature given as:

$$\theta_D = \hbar(6\pi^2 V^{1/2} n)^{\frac{1}{3}} f(\sigma) \sqrt{\frac{B_s}{k_B^2 M}} \quad (1)$$

Where V , M , n , B_s , $f(\sigma)$ and k_B are the molar volume, the molar mass, the number of atoms per formula unit, the adiabatic bulk modulus, a scaling function that depend on Poisson's ratio of the isotropic solid, and the Boltzman constant, respectively. A simple way to use the Debye model is to consider that the adiabatic bulk modulus is equal to the isothermal bulk modulus, B_T , leading to the following equation:

$$B_s \approx B_T = V \left(\frac{d^2 E}{dV^2} \right) \quad (2)$$

Where E is the total energy of the crystal at 0 K. Being given the energy of the considered phase (E) as a function of the molecular volume (V) by means of the FP-LAPW method at static condition ($T = 0$ K), the quasi-harmonic Debye model allows: (i) to generate the Debye temperature $\theta_D(V)$ from Eq. (1) and Eq. (2), (ii) to obtain the non-equilibrium Gibbs function $G^*(V;p,T)$:

$$G^*(V;T,p) = E(V) + pV + A_{vib}(T,\theta(V)) \quad (3)$$

where A_{vib} is the vibrational Helmholtz free energy given by the Debye model, and (iii) to minimize G^* to derive the thermal equation of state (EOS), $V(p,T)$

and the chemical potential $G(p, T)$ of the corresponding phase³¹. The standard thermodynamic relations that depend on temperature and pressure are used to derive other macroscopic properties. A detailed description of this procedure can be found in Ref [32] and references therein.

3. Results

3.1 Structural and electronic properties of $\text{Cr}_2\text{Zr}_{1-x}\text{Nb}_x$ alloys

As a first step, a set of total energy calculation versus total volume, $E (V)$, for $\text{Cr}_2(\text{ZrNb})$ alloys was carried out in order to determine the structural parameters. The corresponding values are fitted with universal Murnaghan equation of state (EOS). The obtained results for Cr_2Zr and Cr_2Nb compounds are presented in Table 1. As it can be seen, the predicted lattice parameters are consistent with those measured experimentally by X-Ray diffraction (room temperature) as well as with those calculated from theoretical methods. The same good agreement is noticed for the bulk moduli for which one can notice that Cr_2Nb is less compressible than Cr_2Zr .

The variation of lattice parameters and bulk moduli with the Nb concentration (x) is represented in Fig. 1(a) and 1(b), respectively. The lattice parameter of $\text{Cr}_2\text{Zr}_{1-x}\text{Nb}_x$ alloys decreases with increasing Nb concentration, whereas the bulk modulus increases. The noticed linear variations of the lattice parameters and the bulk modulus with the Nb concentration indicate that the Vegard's law is valid for these alloys. The deviation from the linearity -that would be represented by a *bowing factor* describing the structural disorder in the alloys- is not present; showing thereby that the $\text{Cr}_2(\text{ZrNb})$ alloys are quite ordered in the entire range of composition whatever the Zr/Nb ratio.

The heats of formation of the studied alloys are determined as the difference of the C15 total energy and the sum of the *bcc*-Cr, *hcp*-Zr, and *bcc*-Nb energies. Figure 2 shows the dependence of the heat of formation with the Nb concentration (x). The obtained values are always negative, meaning that the formation of the C15-alloys is favored to the phase separation. Moreover, starting with Cr_2Zr , the heat of formation decreases with x from 0 to 50 % Nb. In a similar manner, starting with Cr_2Nb , the heat of formation decreases when Nb content is reduced from 100 to 50 %; the lowest value being obtained for 50 Zr and 50 Nb %. These are interesting results indicating that substitution of Zr on

Nb sites in Cr_2Nb or Nb on Zr sites in Cr_2Zr does not destabilize the C15 structure. This is consistent with the recent determination of the 1573 K isothermal section of ternary phase diagrams established by Kim *et al*³⁸. Indeed, the authors found that the Laves phase along the Cr_2Zr - Cr_2Nb pseudo-binary line is composed of the C15 phase over the entire compositional range.

Another way to clarify the structural stability and the hardness of the $\text{Cr}_2(\text{Zr}, \text{Nb})$ alloys is the determination of their electronic structures.

Fig. 3 represents the total (DOS) and partial (PDOS) densities of states in the cases of Cr_2Zr , $\text{Cr}_2\text{Zr}_{0.5}\text{Nb}_{0.5}$, and Cr_2Nb . All the DOS curves present two sets of peaks separated by the Fermi level localized in the vicinity of a quite pronounced valley (deep minimum). The first set of peaks (in the low energy range) corresponds to the valence states whereas the second one (in the high energy range) represents the conduction states. The well-defined valley separating the bonding and antibonding states and the localisation of the Fermi level at the bonding-antibonding valley, was already reported in the literature for Cr_2Zr ³⁴ and Cr_2Nb ³⁹. Let us now focus our interest only on the first set of peaks, since the second one is not well reproduced within the framework of the DFT which fails in dealing with excited states. The results in Fig. 3 indicate the metallic character in all these materials as well as the effect of the Zr/Nb concentration on the density and location of the Fermi level. The DOS at the Fermi level, $N(E_F)$, is 47.32, 51.80, and 115.52 States/Ry for Cr_2Zr , $\text{Cr}_2\text{Zr}_{0.5}\text{Nb}_{0.5}$, and Cr_2Nb , respectively. The $N(E_F)$ of the Cr_2Nb compound is higher than the Cr_2Zr one by more than a factor of 2. Note that our value for Cr_2Nb compares very well with the 115.8 states/Ry given by Ormeci *et al*³⁹. The deep minimum of the DOS is at the right of the Fermi level in Cr_2Nb and quite displaced to the left in Cr_2Zr . In fact, as illustrated in Fig. 3 for the case of $\text{Cr}_2\text{Zr}_{0.5}\text{Nb}_{0.5}$, all the results for the Cr-Zr-Nb Laves phase investigated here showed a displacement of the Fermi level from the left to the right with increasing the Nb concentration. Clearly, the contribution of the Nb and the Zr atoms to the total DOS are quite

different. In lower energies (full states), the PDOS profiles show that the Nb *d*-states contribution is more important than the Zr *d*-states. This confirms that the hybridization between Cr and Nb atoms is effectively more important than the hybridization between Cr and Zr ones. This leads to higher potential hardness in the Cr-rich compounds, as already established from the bulk moduli (see Fig. 1(b)). From the electronic structures, it can be assumed that the ternary compounds $\text{Cr}_2(\text{Zr}_x\text{Cr}_{1-x})$ in the C-15 Laves phase are more stable for Zr-rich concentration. This is consistent with the heats of formation that were previously shown in Fig. 2.

3.2 Thermal properties

Using a given set of total energy versus molar volume values, $E(V)$, and a numerical EOS, the thermal properties are obtained for each alloy. As the Debye temperature in this model depends on the scaling function $f(\sigma)$ (see Eq. (1), in Sec. 2)), values of the Poisson's ratios have to be introduced. In the literature, the reported Poisson's ratios are 0.32³⁵ and 0.34^{40, 41} for Cr₂Zr and Cr₂Nb, respectively. These values are used in the present work and an averaged value of 0.33 is taken for the Cr₂(ZrNb) alloys.

The lattice parameters and bulk moduli obtained with a numerical EOS, at $T = 0$ K (static case) for $x = 0, 0.25, 0.50, 0.75, 1.0$, are 7.138, 7.086, 7.039, 6.992, 6.945 Å and 177.84, 191.47, 204.18, 218.1, 226.04 Gpa, respectively. These results are in fairly good agreement with the Murnaghan EOS and the experimental results (*see* Table 1 and Fig. 1).

Since the C15-phases studied here exist only in the lower temperature range of the Cr₂(Zr, Nb) solids, the thermal properties are determined in the temperature range from 0 to 1500 K, where the quasi-harmonic model remains fully applicable. The temperature effects on lattice parameters and bulk moduli are shown in Fig. 4(a) and Fig. 4(b), respectively. The lattice parameter of each alloy increases with increasing temperature but the rate of increase is more important for Cr₂Zr above 600 K. In terms of bulk modulus (Fig. 4(b)), there are clearly three categories of behavior. The effect of temperature on Cr₂Nb is very moderate as the bulk modulus at 1500 K is still above 220 Gpa. For the Laves phases containing both Zr and Nb, the decrease in bulk modulus with temperature is more drastic. Finally, for the Cr₂Zr alloy the B value drops by more than 40 % between 0 and 1500 K. This indicates that Cr₂Nb stays a hard material at high temperature when compared to Cr₂Zr. A very interesting point about these results is the fact that, as the rate of decrease does not appear to be dependent on the amount of Zr in the Cr-Zr-Nb Laves phases (Fig. 3(b)), small amounts of Nb should be sufficient to improve significantly the hardness of the

Cr₂Zr compound. This interesting behavior was already related to the strong hybridization between Cr and Nb atoms in Sec 3.1.

Other properties which are related to the thermal effects are the thermal expansion, $\alpha(T)$, and the heat capacity, $C_V(T)$. As these two properties have anharmonic behaviors, one would not expect linear variation with Zr/Nb ratio. Fig. 5(a) represents the variation of the (volume) expansion coefficient, $\alpha(T)$, as function of the temperature. After a sharp increase up to ~ 300 K which is due the electronic contributions and is roughly similar for all compositions, the behavior of the Cr₂Nb, Cr₂Zr, and Cr₂(ZrNb) alloys are somehow quite different between 300 and 1500 K. As it can be shown, the Cr₂Nb alloy has a fairly constant thermal expansion. Comparatively, the expansion coefficient of Cr₂Zr exhibits a parabolic behavior at high temperature. The Cr₂-(Zr, Nb) coefficients exhibit linear dependence with the temperature. The reported values for the Cr₂-(Zr, Nb) alloys are lower and higher than the Cr₂Zr and Cr₂Nb ones, respectively.

Another vibrational property is the heat capacity and its dependence on temperature. The calculated values for the studied alloys are compiled in Table 2. The reported value follows the Debye model at low temperature ($C_V(T) \sim T^3$) and the classical behavior is found at sufficient high temperatures ($C_V(T) \sim 3R$ for mono-atomic solids); obeying Dulong *et* Petit's Rule. The specific heat capacity of the three materials at sufficient high temperature does not dependent much on temperature and tends to approach $75 \text{ J.mol}^{-1}.\text{K}^{-1}$.

The calculated properties at different temperatures are very sensitive to the vibrational modes. In the quasi-harmonic Debye model, the Grüneisen parameter, $\gamma_G(T)$, and the Debye temperature, $\Theta_D(T)$, are two key quantities. In Fig. 5(b), the Grüneisen parameter is plotted for the different temperature values at $p = 0$ Gpa. The Grüneisen parameter decreases with temperature for Cr₂Nb while it increases for Cr₂Zr. The plotted values vary from 1.8 to 2.5, which show that the vibrational modes in Cr₂Nb and Cr₂Zr are quite different

and sensitive to the Zr/Nb ratio in the ternary compounds. The values of the Debye temperature are given in Table 3 for 0, 300, and 600 K. A very good agreement is found for the Cr₂Nb compounds at 300 K between our calculated results and the experimental data of Thoma *et al*⁴². Though the calculated value obtained by Mayer *et al*³³ for Cr₂Nb is higher than these results, the fact that they found a lower Debye temperature for Cr₂Zr compared to Cr₂Nb is consistent with our values. It is well known that hard materials exhibit elevated Debye temperatures. This is the case for the Cr₂Nb and Cr₂Zr compounds for all the temperature range. Finally, our calculations give fairly accurate estimation of the Debye temperatures and depict well its evolution in Cr₂(Zr, Nb) alloys. The trend is to increase with the Nb concentration and to decrease with temperature.

4. Conclusion

The aim of this work was to use *ab initio* calculations (with the FP-LAPW method) to give new insights on structural, electronic, and thermal properties of binary and ternary C15-Laves compounds in the Cr-Zr-Nb system. The temperature effects have been obtained using the quasi-harmonic Debye model exploiting the total energy calculations of the FP-LAPW method. The main results can be summarized as follows:

1. The calculated lattice parameter and bulk modulus of Cr_2Zr and Cr_2Nb are in good agreement with experimental data. The lattice parameters of the $\text{Cr}_2(\text{Zr}, \text{Nb})$ compounds decreases with Nb concentration, whereas the bulk modulus increases.
2. The calculated heats of formations show that the Cr-Zr-Nb system favors ternary C15- $\text{Cr}_2(\text{Zr}, \text{Nb})$ compounds formation over phase separation. In addition, the structural properties obey to the Vegard's law, meaning that $\text{Cr}_2(\text{Zr}, \text{Nb})$ are quite ordered alloys whatever the Zr/Nb ratio.
3. The total densities of states have shown that the stability of the ternary Laves compound $\text{Cr}_2(\text{Zr-Nb})$ decreases with increasing the Nb content. The partial densities of states (*d*-states) of the Nb atoms are more important than the Zr ones in the low energy range. This leads to a strong hybridization between Nb and Cr *d*-states.
4. Bulk modulus values as well as the type of hybridization between Cr-Nb and Cr-Zr suggest higher hardness potential for Cr_2Nb than for $\text{Cr}_2(\text{Zr}, \text{Nb})$, and finally for Cr_2Zr .
5. The use of the quasi-harmonic Debye model was successfully applied to determine the thermal properties of the $\text{Cr}_2(\text{Zr}, \text{Nb})$ alloys in the 0-1500 K temperature range. Significant differences in properties are obtained Above 300 K.

6. The behavior of the Laves phases in Cr-Zr-Nb system is very sensitive to the Zr/Nb ratio. Our results indicate that the effects of temperature on bulk moduli and volume expansions are very drastic in Cr_2Zr and less important in Cr_2Nb .

Finally, the approach presented here is a promising alternative for the determination of several properties in complex structures that are difficult and/or costly to obtain from experiments.

Table captions

Table 1. Lattice constant (a) and bulk modulus (B) of Cr_2Zr and Cr_2Nb in the C15-Laves phase.

	a (Å)	B (Gpa)
Cr₂Zr		
Present work	7.131	177
<i>Ref</i>³³	7.093	179
Experiment	7.208 ³⁴	162 ³⁵
Cr₂Nb		
Present work	6.940	228
<i>Ref</i>³³	6.918	229
Experiment	6.991 ³⁶	229 ³⁷

Table 2. The heat capacity C_v (J. /mol. K) at different temperatures.

	300 K	600 K	900 K
Cr_2Zr	67.77	73.04	74.06
$\text{Cr}_2\text{Zr}_{0.75}\text{Nb}_{0.25}$	67.81	73.04	74.05
$\text{Cr}_2\text{Zr}_{0.50}\text{Nb}_{0.50}$	67.42	72.94	74.01
$\text{Cr}_2\text{Zr}_{0.25}\text{Nb}_{0.75}$	66.99	72.81	73.95
Cr_2Nb	66.89	72.78	73.93

Table 3. The Debye temperature θ_D (K) for the Cr-Zr-Nb system at 0, 300, and 600 K.

	0 K	300 K	600 K
Cr ₂ Zr	431.0	426.7 437 ³³	417.9
Cr ₂ Zr _{0.75} Nb _{0.25}	429.5	425.4	418.6
Cr ₂ Zr _{0.50} Nb _{0.50}	441.9	437.9	430
Cr ₂ Zr _{0.25} Nb _{0.75}	455.3	451.5	444.7
Cr ₂ Nb	458.2	454.6 502 ³³ 453.9 ⁴²	448.4

References

- ¹ Goldshmidt HJ, Brand JA. *J. Less-Common Met.* 1961; 3:44.
- ² Taub A, Flesher L. *Science* 1989; 243:616.
- ³ Anton DL, Shah DM. *Mater. Sci. Eng. A* (1992); 153:410.
- ⁴ Livingston JD, Briant CL. In *High-temperature silicides and refractory alloys*. Petrovic JJ, Bewlay BP, Vasudevan AK, Lipsitt HA (eds). Pittsburgh (PA): MRS1994; p.p. 395.
- ⁵ Kumar KS. In *High-temperature ordered intermetallic alloys VII*. Koch CC, Liu CT, Stolof NS, Wanner A (eds). Pittsburgh (PA): MRS1997; pp 677.
- ⁶ Cook JA, Liaw PA, Liu CT, Bhaduri SB. In *The Johannes Weertman Symposium*. Arsenault RJ, Cole D, Gross T, Kostoroz G, Liaw P, Parameswaran S, Sizek H (Eds.). TMS Warrendale PA 1996, pp 47.
- ⁷ Kumar KS, Liu CT. *Acta. Metall. Mater.* 1997; 45:3671.
- ⁸ Chen KC, Allen SM, Livingston JD. In *High temperature ordered intermetallic alloys VI*, Horton J et al. (eds). Pittsburgh (PA): MRS1995; pp 1401.
- ⁹ Thoma DJ, Perepezk JH. *Mater. Sci. Eng. A* (1992); 156:97.
- ¹⁰ Takasugi T, Yoshida M, Hanada S. *Mater. Sci. Eng. A* 1995; 192/193:805.
- ¹¹ Bewlay BP, Sutli JA, Jackson MR, Lipsitt HA. *Acta. Metall. Mater.* 1994; 42:2869.
- ¹² Anderson KR, Groza JR, Dreshreld RL, Ellis D. *Metall. Mater. Trans. A* 1995; 26:2197.
- ¹³ Hong S, Fu CL, Yoo MH. *Phil. Mag. A* 2000; 80:871.
- ¹⁴ Jackson MR, Rowe RG, Skelly DW. In Horton JA, Baker I, Hanada S, Noebe RD, Schartz DS (eds.). *High Temperature Ordered Intermetallic alloys VI*, Vol 364, MRS Publication, Pittsburg, PA, 1995, pp.1339-44.
- ¹⁵ Livingston JD. *Phys. Stat. Sol.* 1992; 131:415.
- ¹⁶ Hazzledine PM, Pirouz P. *Scr. Metall.* 1993; 28:1277.
- ¹⁷ Kazantzis AV, Aindow M, Jones IP. *Mat. Sci. Eng. A* 1997; 223:44.
- ¹⁸ Liu CT, Tortorelli PF, Horton JA, Carmichael CA. *Mat. Sci. Eng. A* 1996; 214:23.
- ¹⁹ Hong S, Fu CL. *Intermetallics* 1999; 7:5
- ²⁰ Lee S, Liaw PK, Liu CT, Chou YT. *Mat. Sci. Eng. A* 1999; 268:184.
- ²¹ Brady MP, Zhu JH, Liu CT, Tortorelli PF, Walker LR. *Intermetallics* 2000; 8:1111.
- ²² Hong S., Fu CL. *Intermetallics* 2000; 9:799.

- ²³ Hong S, Fu CL. Phys. Rev B 2002; 66:094109
- ²⁴ Takasugi T, Kumar KS, Liu, CT, Lee EH. Materials Science and Engineering A 1999; 260:108.
- ²⁵ Kumar KS, Miracle DB. Intermetallics 1994; 2:257.
- ²⁶ Kumar KS, Pang L, Horton JA, Liu CT. Intermetallics 2003; 11:677.
- ²⁷ Stein F, Palm M, Sauthoff G. Intermetallics 2004, In Press, Corrected Proof..
- ²⁸ Blaha P, Schwartz K, Luitz J., WIEN2k, Vienna University of Technology, (1997). Blaha P, Schwartz K, Sorantin P, Trickey SB. Comput. Phys. Commun. 1990; 59:399.
- ²⁹ Perdew JP, Chevary JA, Vosko SH, Jackson KA, Pederson MR, Singh DJ, Fiolhais C. Phys. Rev. B 1992; 46:6671; Perdew JP, Burke K, Ernzerhof M. Phys. Rev. Lett. 1996; 77:3865.
- ³⁰ Zhu JH, Liu CT, Liaw PK. Intermetallics 1999; 7:1011.
- ³¹ Maradudin AA, Montroll EW, Weiss GH, Ipatova IP. Theory of Lattice Dynamics in the Harmonic Approximation, Academic Press 1971.
- ³² Blanco MA, Francisco E, Luaña V. Computer Physics Communications 2004; 158 :57.
- ³³ Mayer B, Anton H, Bott E, Methfessel M, Sticht J, Harris J, Schmidt PC. Intermetallics 2003; 11:23.
- ³⁴ Villars P, Calvert LD. Pearson's handbook of crystallographic data for intermetallic phases, vol. 2. Metals Park, OH: ASM 1985 ; p. 1908.
- ³⁵ Foster K, Hightower JE, Leisure RG. Phil. Mag. B 2000; 80:1667.
- ³⁶ Thomas DJ, Perepezko JH. Mater. Sci. Eng. A 1992; 136:61.
- ³⁷ Chu F, He Y, Thoma DJ, Mitchell TE. Scripta Metallurgica et Materialia 1995; 33:1295.
- ³⁸ Kim WY, Takasugi T. Scripta Materialia 2003; 48-559.
- ³⁹ Ormeci A, Chu F, Wills JM, Mitchell TE, Albers RC, Thoma DJ, Chen SP. Phys. Rev. B 1996; 54:12753.
- ⁴⁰ Chu F, Mitchell TE, Chen SP, Sob M, Siegl R, Pope DP. In High Temperature Structural Intermetallic Alloys-VI. Horton J, Baker I, Hanada S, Noebe D. MRS 1995; pp 1389.
- ⁴¹ Chen KC, Chu F, Kotula PG, Thoma DJ. Intermetallics 2001; 9:785.
- ⁴² Thoma DJ, Chu F, Peralta P, Kotula PG, Chen KC, Mitchell TE, Materials Science and Engineering A 1997; 239-240:251.

List of figures

Fig. 1 Variation with Nb concentration (x) of (a) the lattice parameter and (b) the bulk modulus.

Fig. 2 Variation of the heat of formation versus Nb concentration, x .

Fig. 3 Total (DOS) and partial (PDOS of d -states) densities of states of C15-Cr₂Zr, -Cr₄ZrNb, and -Cr₂Nb Laves structures. The dashed vertical line refers to the Fermi level.

Fig. 4 Variation with the temperature at $p=0$ of (a) the lattice parameters and (b) the bulk moduli.

Fig. 5 Variation with the temperature at $p=0$ of (a) the thermal expansion and (b) the Grüneisen parameter

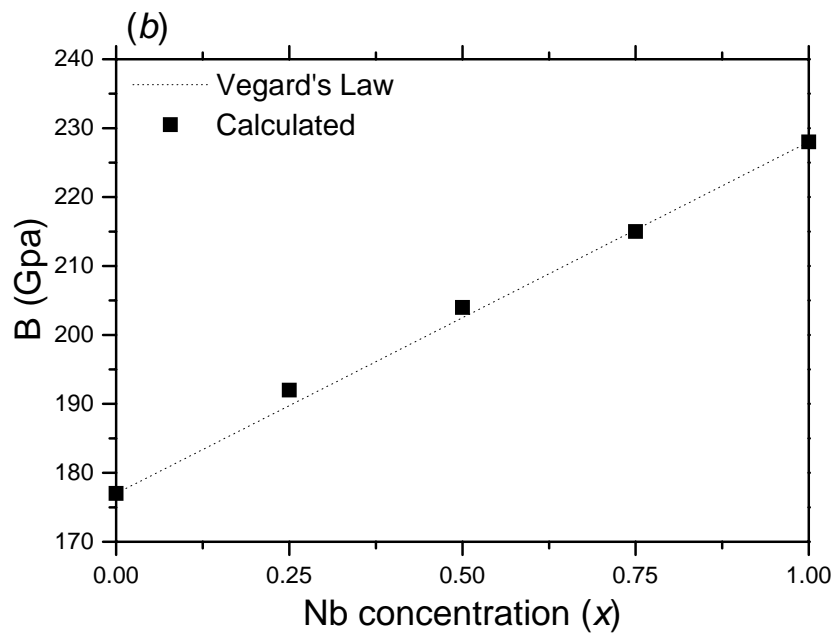
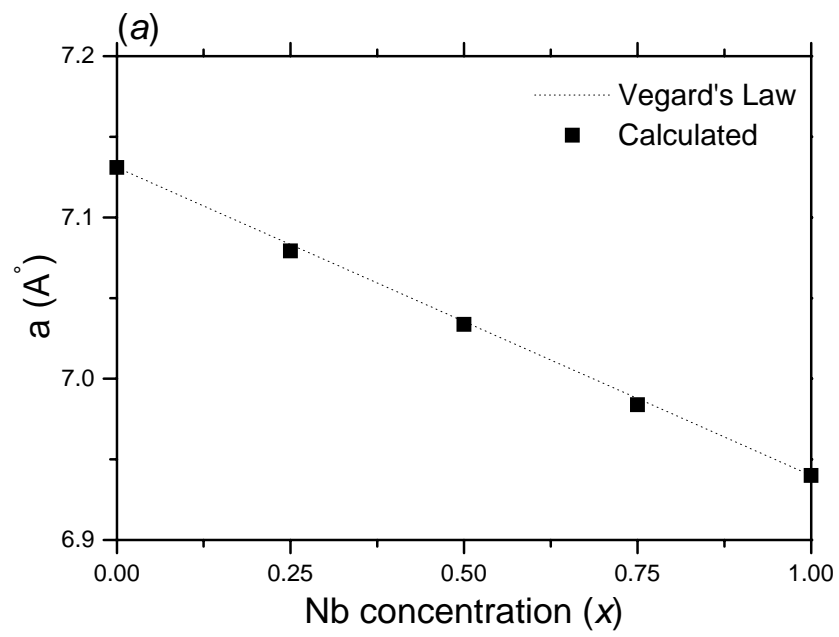


Figure 1

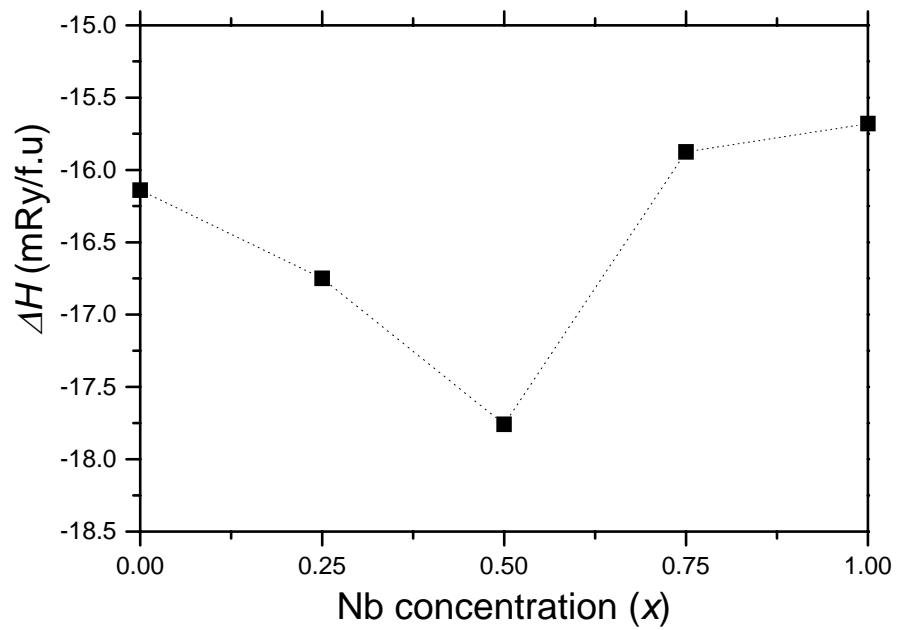


Figure 2

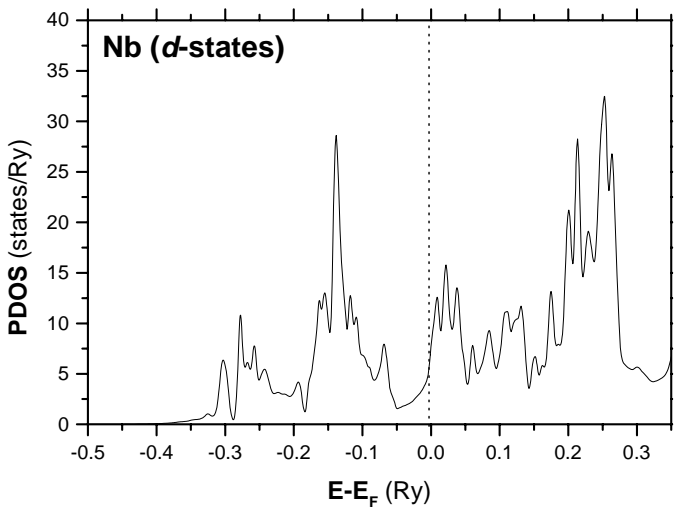
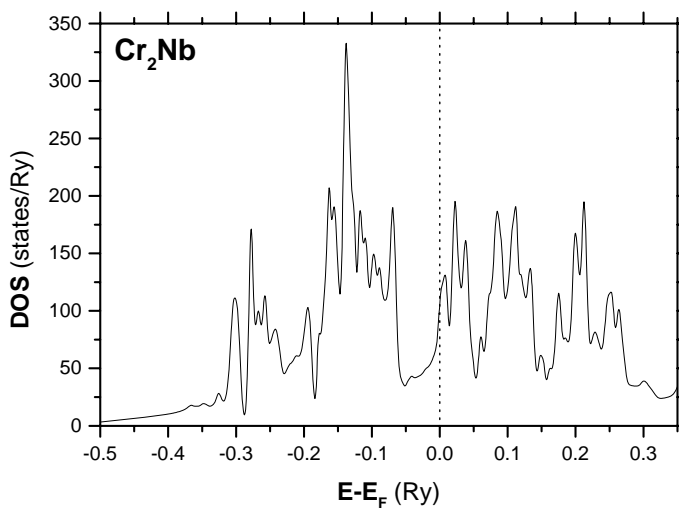
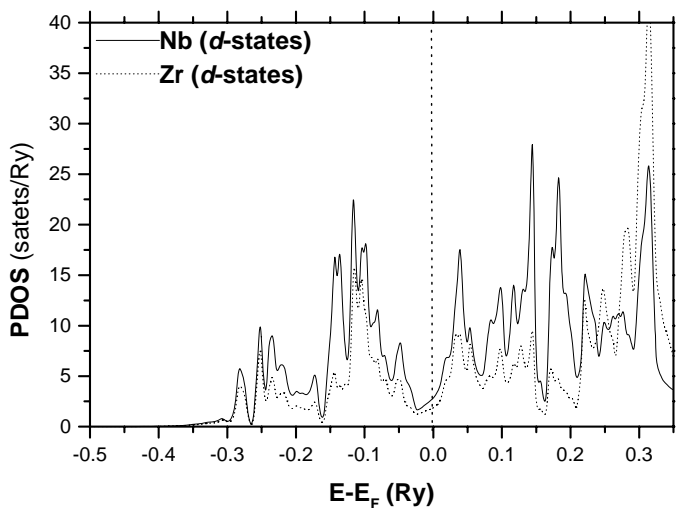
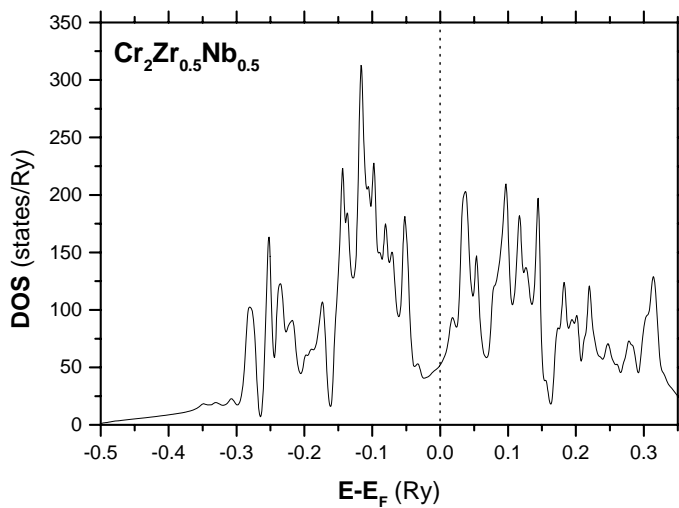
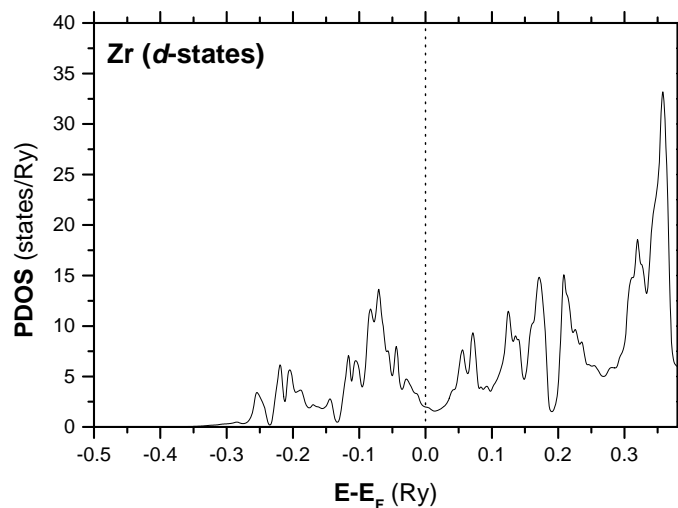
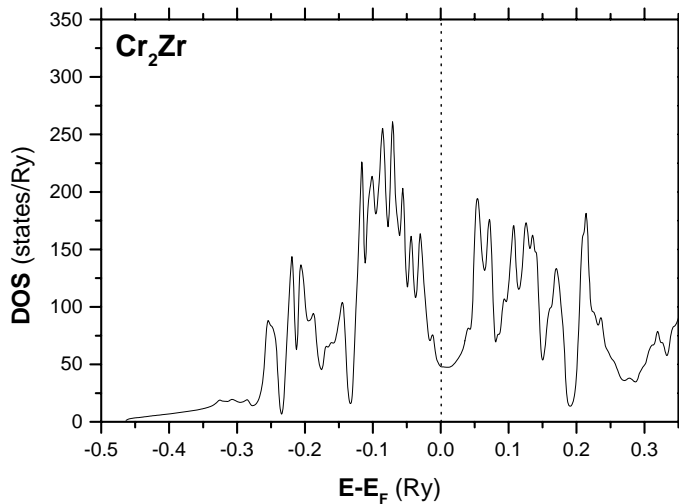


Figure 3

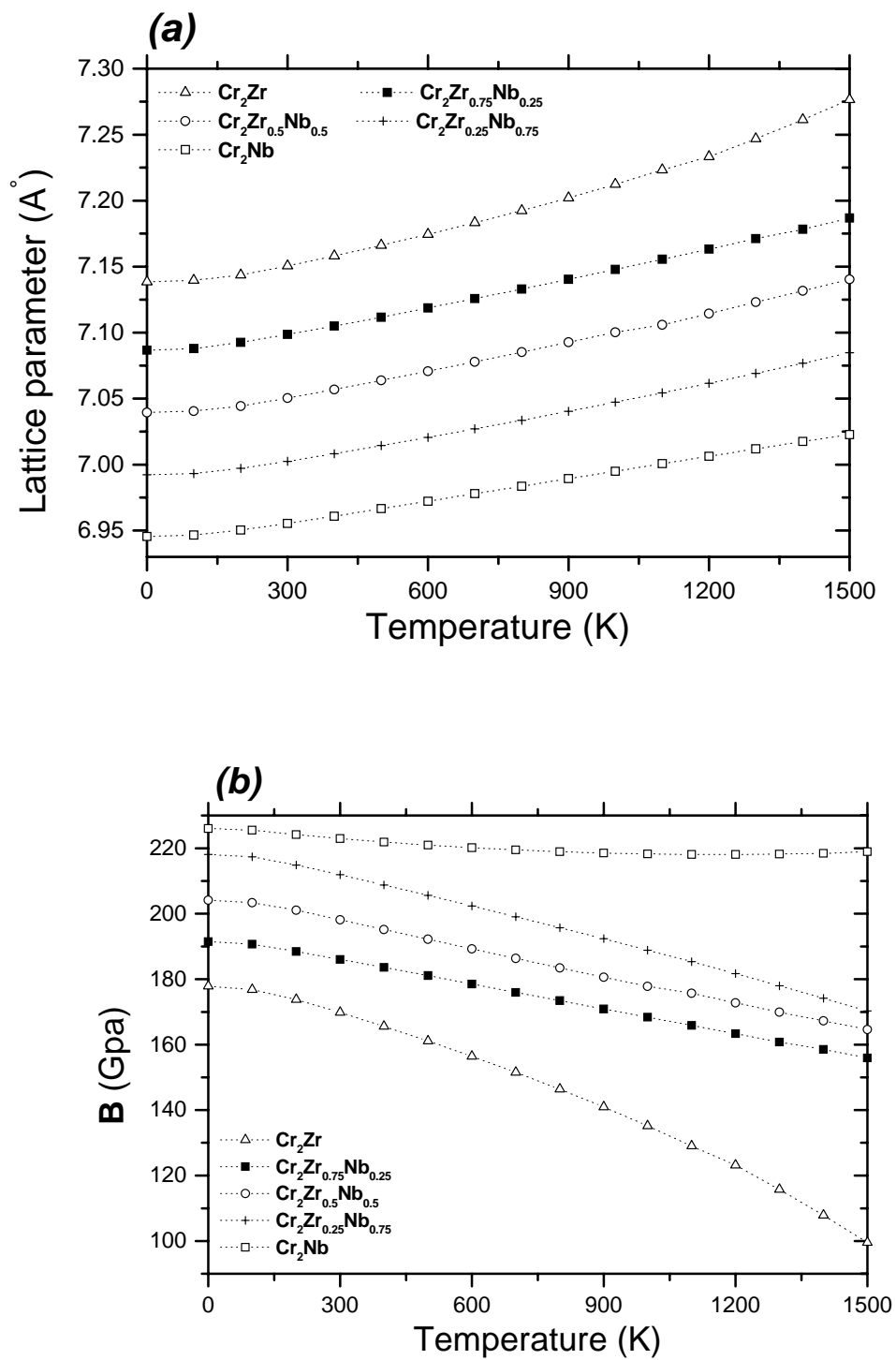


Figure 4

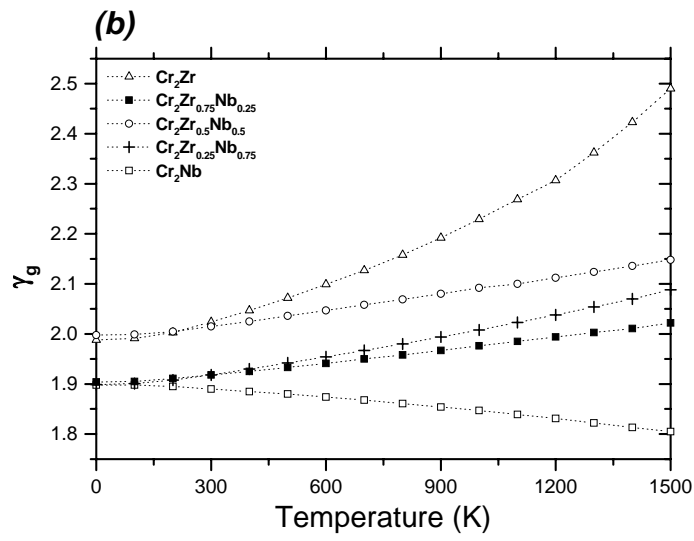
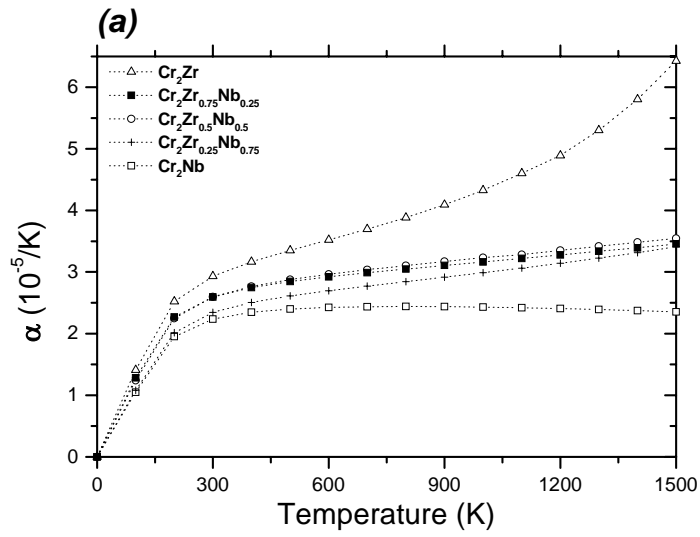


Figure 5